Study of the Fine Structure in the High-Field Galvanomagnetic Properties and the Fermi Surface of Copper

J. R. KLAUDER, W. A. REED, G. F. BRENNERT, AND J. E. KUNZLER
Bell Telephone Laboratories, Inc., Murray Hill, New Jersey
(Received 31 August 1965)

Extensive high-field galvanomagnetic data for high-purity single crystals of copper are reported and analyzed in terms of current theory. Special attention is given to the study and identification of the higher order open orbits, commonly called "whiskers," and to an understanding of their presence and extent. Accurate measurements of the Hall constant for the field orientations ⟨111⟩ and ⟨100⟩ were made and values significantly different from those reported earlier were obtained. Our experimental results are in good agreement with theoretical predictions based on Roaf's best phenomenological Fermi-surface model (CU VI).

I. INTRODUCTION

IN this paper, we present a portion of our extensive high-field galvanomagnetic data on high-purity single crystals of copper and present the interpretation of our data in terms of current theory. Our data exhibit not only the principal magnetoresistance behavior of peaks and ridges reported earlier by Kunzler and Klauder,[1] and independently by Alekseevskii and Gaidukov,[2] but also they contain a veritable wealth of minor magnetoresistance peaks associated with higher order open orbits, a few of which were reported earlier.[3] We concentrate a good deal of our attention on this "fine structure" and its explanation in terms of the Fermi surface of copper. This analysis is greatly aided by the use of the transverse-even voltage, which permits the determination of open-orbit directions from measurements made for a single magnetic-field orientation.[4] These results support our earlier conclusions[3] that the higher order open orbits, coupled with Hall-constant measurements, provide critical "calipers" on possible Fermi-surface models. This contention is supported in the present paper with numerical comparison between our results and two models of the Fermi surface of Cu: that put forward by Pippard[5] (in the form proposed by Garcia-Moliner[6]) and that suggested more recently by Shoenberg[7] (in one of the several forms proposed by Roaf[8]). We find quite good agreement with Roaf's best results, denoted by CU VI.

It has long been recognized that high-field magnetoresistance and Hall-effect data contained important information regarding Fermi surfaces of metals, which is not only qualitative but also quantitative as well.[9] However, an understanding of these phenomena was not forthcoming until the advent of the phenomenological theories of Lifshitz, Azbel, and Kaganov[10] (LAK) and of Lifshitz and Peshanskii[11] (LP). When these theories are applied to uncompensated metals in the high-field region, the quadratic dependence on magnetic field of the magnetoresistance for certain field orientations is to be understood purely geometrically, arising from open orbits supported by the Fermi surface (FS) rather than depending sensitively on the nature of the relaxation phenomena. Thus, information of a geometrical nature regarding the FS can be obtained from the magnetoresistance data, which is one of our purposes here. Early investigations[1,2] based on these theories concentrated on the noble metals, in part because of their availability at that time as high-purity single crystals, and in part because of their comparatively simple FS. However, care must be taken in interpreting the magnetoresistance data even for a simple FS as it is not unambiguously linked to the FS geometry. That care is necessary was borne out in early interpretations for Cu, where the initial interpretation[2] was at variance with the model proposed by Pippard,[5] and where subsequent interpretations by two of us[1,3] and independently by Priestly[12] showed confirmation of the basic Pippard model.

Since that time, the galvanomagnetic properties of a large number of metals, including may of the transition metals, have been investigated. A summary of this work is afforded by the review article of Fawcett.[13] A good deal of this work has been of a survey nature, rather than being detailed, in an attempt to deduce the topology and gross topographical features of the Fermi surfaces, many of which are very complicated multi-sheeted affairs. Such an over-all view is presently a reasonable procedure for such complex metals, but more definitive studies are appropriate for Cu at this stage.[14]

[1] J. E. Kunzler and J. R. Klauder, Bull. Am. Phys. Soc. **5**, 150 (1960).
[2] N. Alekseevskii and Yu. Gaidukov, Zh. Eksperim. i Teor. Fiz. **36**, 447 (1959) [English transl.: Soviet Phys.—JETP **9**, 311 (1959)].
[3] J. R. Klauder and J. E. Kunzler, *The Fermi Surface*, edited by W. A. Harrison and M. B. Webb (John Wiley & Sons, Inc., New York, 1960), p. 125.
[4] J. R. Klauder and J. E. Kunzler, Phys. Rev. Letters **6**, 179 (1961).
[5] A. B. Pippard, Phil. Trans. Roy. Soc. **A250**, 325 (1957).
[6] F. Garcia-Moliner, Phil. Mag. **3**, 207 (1958).
[7] D. Shoenberg, Phil. Trans. Roy. Soc. **A255**, 85 (1962).
[8] D. J. Roaf, Phil. Trans. Roy. Soc. **A255**, 135 (1962).
[9] M. Kohler, Ann. Physik **5**, 99 (1949).
[10] I. M. Lifshitz and M. I. Azbel,. M, I. Kaganov, Zh. Eksperim. i Teor. Fiz. **31**, 63 (1956) [English transl.: Soviet Phys.—JETP **4**, 41 (1957)].
[11] I. M. Lifshitz and V. G. Peschanskii, Zh. Eksperim. i Teor. Fiz. **35**, 1251 (1958); **38**, 188 (1960) [English transl.: Soviet Phys.—JETP **8**, 875 (1959); **11**, 137 (1960)].
[12] M. G. Priestley, Phil. Mag. **5**, 111 (1960).
[13] E. Fawcett, Advan. Phys. **13**, 139 (1964).
[14] Our data are consistent with those reported by A. J. Funes and R. V. Coleman, Phys. Rev. **131**, 2084 (1963); R. V. Coleman, A. J. Funes, J. S. Plaskett, and C. M. Tapp, Phys. Rev. **133**, A521 (1964). However, these authors do not discuss properties of the higher order open orbits or Hall effect.

Section II is devoted to a description of the experimental procedures and apparatus and to our Cu samples with which our data was obtained. We have made extensive use of a sample holder that permits an arbitrary orientation of the sample in space. This holder is used in conjunction with an electromagnet, with a maximum field of 18 kOe, which may be rotated through an angle of 180°. The combination of holder and magnet enables, essentially, every field orientation to be obtained with a single sample. This feature has permitted numerous cross checks on our data between points of equivalent crystal symmetry. A representative portion of our data is presented in Sec. III along with several stereographic representations of the observed magnetoresistance "ridge," "valley," and "volcano-like" behavior, shown in Fig. 8, and in more clarity and detail in Fig. 9. These data exhibit the principal magnetoresistance ridges associated with open orbits along ⟨111⟩, ⟨100⟩, and ⟨110⟩ directions, which have been reported earlier. In addition, "whiskers," i.e., lesser magnetoresistance ridges (arcs of great circles), are associated with still higher order open orbits along ⟨113⟩, ⟨133⟩, ⟨112⟩, ⟨122⟩, ⟨115⟩, ⟨155⟩, ⟨335⟩, ⟨355⟩, ⟨223⟩, ⟨233⟩, ⟨012⟩, ⟨013⟩, ⟨015⟩, ⟨023⟩, ⟨035⟩, and ⟨123⟩ directions. Arcs associated with these orbits extend as much as 20° away from a symmetry axis, or as little as a few degrees beyond the two-dimensional region. There is even evidence for a "fuzz" on each of the two-dimensional regions corresponding to an exceedingly large number of still higher order open-orbit directions for which the ridge exists for only a fraction of a degree outside the two-dimensional region. For the most part, such "fuzz" is too extensive and of too weak a nautre to be of experimental significance. However, the existence of the "fuzz" is in full agreement with theoretical interpretations and is indicative of the high purity and crystalline perfection of our sample.

In Sec. IV, we present an analysis and a theoretical interpretation of our data and relate it to various features of the FS. Numerical confirmation between experiment and theory is sought for several aspects of the data governed by geometrical properties alone. These include the Hall constants along the ⟨100⟩ and ⟨111⟩ directions. Values of these constants were previously reported,[3,15] but our present values differ from our earlier ones for both orientations. One source of these differences is found in our earlier evaluation method, which was to divide the Hall voltage by the field, at the maximum field value. More accurate evaluation is attained if, at the maximum field, the *slope* of the voltage versus field curve is used, as this more nearly approximates the high-field limit. A re-evaluation of the earlier data following this procedure supports the present data for the ⟨100⟩ directions. However, another modification exists for the Hall constant appropriate to ⟨111⟩ directions due to the extraordinary sensitivity of the measurements to magnetic-field orientation in that region. By "searching" the vicinity of a ⟨111⟩ direction for the maximum Hall voltage and by considering results from numerous measurements, we believe we have overcome the orientation-sensitivity problem and have attained a reasonably reliable Hall constant for the ⟨111⟩ directions. Comparative experimental and theoretical data are summarized in Table III.

Finally, attention is devoted to the interpretation of the numerous higher order open orbits and to the influence on the FS shape due to their presence and angular extent. The shape and features of one of the strongest such open orbits—those along ⟨113⟩ directions—is analyzed in some detail. These various aspects of our data are analyzed with the aid of phenomenological FS's for Cu and a computer program described elsewhere.[16]

II. EXPERIMENTAL PROCEDURES

A. Sample Preparation and Mounting

All measurements reported in this paper have been made on one sample, although some measurements were made on other samples in order to check parts of the data. The sample was cut with an acid string saw from a single-crystal boule,[17] and then acid-lapped into a rectangular bar with dimensions 2.31 mm wide by 2.54 mm thick by 15.88 mm long. The measured residual resistance ratio is 8000. The orientation was measured with an x-ray defractometer and the long axis of the sample and the [110] crystal axis were aligned to within one degree. The orientation of the crystal and the position and numbering of the potential leads is shown schematically in Fig. 1. The Hall (transverse) leads are soldered in a plane perpendicular to the sample axis, and the magnetoresistance leads are placed parallel to the sample axis so that all three components of the electric field can be measured. The distance between leads is $d_1=7.20$ mm, $d_2=2.31$ mm, and $d_3=2.54$ mm. The crystal is mounted on a Bakelite disk such that the sample and disk could be attached to or removed from the sample assembly without disturbing the sample or the leads connected directly to it.

The sample assembly is constructed so that it can be clamped to the Dewar tail and the crystal rotated $\pm 5°$ about one horizontal axis and $\pm 90°$ about a horizontal axis perpendicular to the first. This allows the sample to be accurately aligned in the magnetic field and rotated from a vertical to horizontal position while the sample is immersed in liquid heluim.

B. Measurement Techniques

The potentials are measured on a Liston-Becker dc amplifier which in the circuit has a sensitivity of 2×10^{-9} V. The output of the amplifier is recorded as a continuous function of either magnetic field intensity or direction on a Moseley 2*S* *x*-*y* recorder. Encoders are attached to both the *x* and *y* axes of the recorder,

[15] J. E. Kunzler and J. R. Klauder, Phil. Mag. **6**, 1045 (1961).

[16] J. R. Klauder, Bell System Tech. J. **40**, 1349 (1961).

[17] E. M. Probansky, Trans. AIME **230**, 925 (1964).

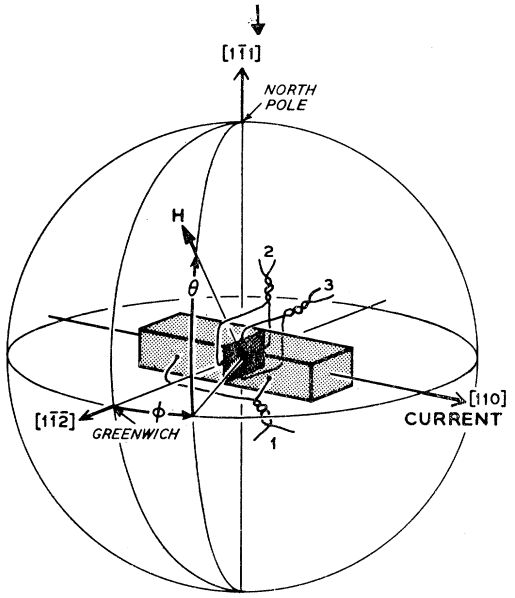

FIG. 1. Schematic representation of copper sample, attached leads, and applied magnetic field. One pair of leads—pair 1—is parallel to the current direction, while the two other pairs of leads—pairs 2 and 3—are transverse to the current. The planes of magnetic field rotation are conveniently described in geodetic terminology on the unit sphere with the "North Pole" located at [1$\bar{1}$1]. Each of our planes of rotation corresponds to a "meridian" of constant "longitude" angle, ϕ, measured "east of Greenwich" which is located at [1$\bar{1}\bar{2}$]. The position of the field **H** in the "meridian" plane is specified by the "latitude" angle, θ, measured "north" of the "equatorial" plane, (1$\bar{1}$1).

and their output punched into paper tape by a Datex data-collecting system. The data on the tapes are then reduced by an IBM 7090 computer, and the final results plotted graphically on microfilm.

The procedure of reversing both current and field directions is used in making the measurements.[18] We define the magnetoresistance voltage (on pair 1) V_{MR} or transverse-even voltage (on pairs 2 and 3) V_{TE} as that component of the measured voltage which reverses sign with current but not with field. The Hall voltage V_H, the parasitic thermal voltage V_T and the induced voltage V_I are similarly defined as odd in both current and field, even in both current and field, and even in current but odd in field, respectively. If we denote a voltage measured with the current direction positive and magnetic field direction negative by $V(+-)$, we then obtain the voltages of interest from the measured voltage by the following relations:

$$V_{\mathrm{MR}} \text{ or } V_{\mathrm{TE}} = \tfrac{1}{4}[V(++)+V(+-)-V(-+)-V(--)],$$
$$V_H = \tfrac{1}{4}[V(++)-V(+-)-V(-+)+V(--)],$$
$$V_T = \tfrac{1}{4}[V(++)+V(+-)+V(-+)+V(--)],$$
$$V_I = \tfrac{1}{4}[V(++)-V(+-)+V(-+)-V(--)].$$

[18] For details see W. A. Reed and J. A. Marcus, Phys. Rev. **126**, 1298 (1962).

The resistive voltage (i.e., that odd in I, even in H), which is observed on pairs 2 and 3, contains in addition to the transverse-even voltage a magnetoresistance voltage due to a small misalignment of the transverse potential pairs. The removal of this "misalignment voltage" is discussed in Sec. IIIB.

A series of rotation curves are taken on all three potential pairs at 4.2°K and in fields of 18 kOe. The magnetic field is rotated along a "meridian" line of constant "longitude" angle, ϕ, measured "east of Greenwich" [1$\bar{1}\bar{2}$](see Fig. 1). Thus, the data consist of continuous tracings of the potential across each pair as a function of the magnetic field "latitude" angle θ. The "longitude" angle ϕ was changed in increments of 2–3° from $\phi=0°$ to $\phi=32°$. Since it is important that the field rotate along a "meridian" which passes through the [1$\bar{1}$1] axis, special care is taken to realign the sample each time the angle ϕ is changed. For the magnetic field parallel to the [00$\bar{1}$], [1$\bar{1}$0], [1$\bar{1}$1], and [1$\bar{1}\bar{2}$] axis, and at various other field directions which appeared interesting, the field dependence of the potentials across all three pairs has also been measured.

III. EXPERIMENTAL OBSERVATIONS AND INTERPRETATIONS

A. General

The measurement procedure described in Sec. IIB results in an enormous quantity of data, all of which is impractical to present. Instead we have selected several curves that are representative and which are useful for illustrating certain points. In addition, we have summarized prominent features of essentially all our data in the conventional stereographic form in which only saturating and nonsaturating behaviors are distinguished. For clarity, our discussion of the observed data is separated into two parts, one belonging to the principal data and one belonging to the fine structure.

B. Principal Data

One of our "meridian" planes is the plane (110) transverse to the current direction and yields data pertinent to several important crystallographic directions. Figure 2 shows the magnetoresistance data in part (a) and the transverse-even voltages in parts (b) and (c). Ideally, in this symmetry plane, these latter two voltages should be identically zero, but they differ from zero for two reasons. First, one notices a gross similarity in shape, although on a reduced scale, between the curves in (b) and (c). This is due to a longitudinal misalignment of the Hall pairs 2 and 3, such that they are not precisely orthogonal to the current direction. This misalignment is not serious, and correction is made by determining from curves such as Fig. 2 the fraction of the pair-1 voltage which appears on pairs 2 and 3, and then subtracting out the fraction of pair 1 from pairs 2 and 3 for each ϕ angle. The second feature is an asymmetry in the

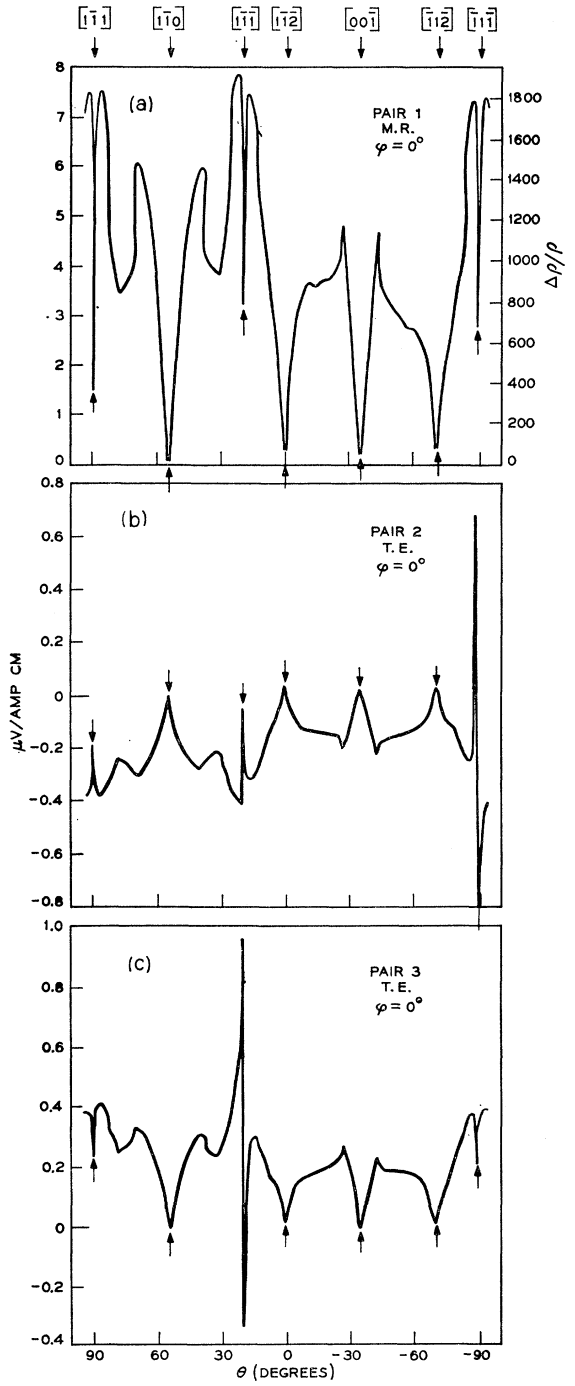

FIG. 2. Resistivity (a) and transverse-even voltages (b) and (c) versus the magnetic field angle θ in the "meridian" plane $\phi=0$. The ordinate is the relevant voltage divided by the sample current and by the separation of the appropriate probes. The magnetoresistance scale is given on the right of part (a). Several important symmetry directions in this plane are indicated at the top of the figure.

figures, particularly a variation in the neighborhood of the various ⟨111⟩ directions. This is due to an imprecise planar rotation of the magnetic field. However, this is indeed a small effect; and only the extraordinary sensitivity which occurs in the ⟨111⟩ directions brings this feature into the open.

The magnetoresistance is generally large ($1–2\times10^3$, at 18 kOe) in this figure, and it varies approximately as H^2. On the other hand, at the minima the magneto-

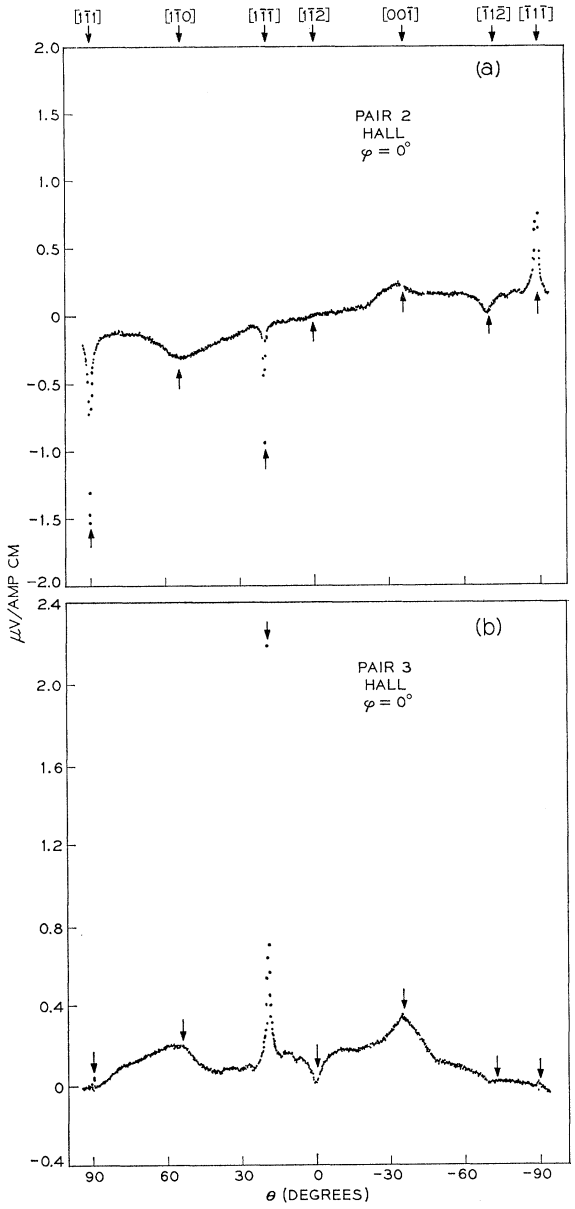

FIG. 3. Hall voltages versus magnetic-field angle in the "meridian" plane $\phi=0°$. The data is presented here in the discrete form arising from the Datex encoders. (a) Pair 2. The signal vanishes at $\theta=0°$ where the field is parallel to the probes. (b) Pair 3. The signal vanishes at $\theta=\pm90°$ where the field is parallel to the probes. The ordinate is the relevant voltage divided by the sample current and by the appropriate probe separation. Note the exceptional sharpness in the vicinity of ⟨111⟩ directions. Repeated runs on expanded scales were necessary to properly define the peak.

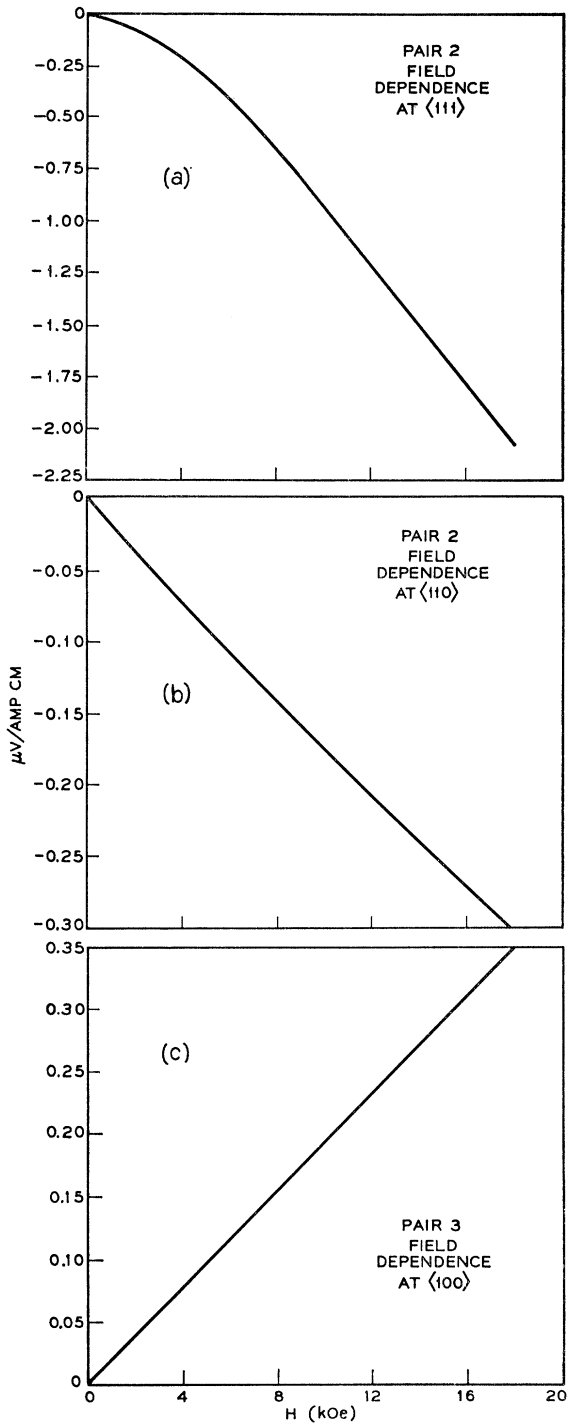

FIG. 4. Hall-voltage field dependences: (a) Pair 2. Hall voltage versus magnetic-field magnitude along $[1\bar{1}1]$ at $\theta=89.4°$, $\phi=0°$. (b) Pair 2. Hall voltage versus magnetic-field magnitude along $[1\bar{1}0]$ at $\theta=54°$, $\phi=0°$. (c) Pair 3. Hall voltage versus magnetic-field magnitude along $[00\bar{1}]$ at $\theta=-35.6°$, $\phi=0°$. Note that the "high-field" region, as indicated by the straightness of the curve, is attained quickly in (b) and (c) and only at about 6 kOe in (a).

resistance is small, and the behavior, comparatively speaking, is one of saturation.

Figures 3(a) and (b) represent the Hall signal in $\mu V/(A$ cm) in the (110) plane for pairs 2 and 3, respectively. The extraordinary sensitivity of the Hall voltage in the ⟨111⟩ directions is readily apparent in these figures. It is tempting to deduce the Hall constant R_H appropriate to the high-field limit directly from Fig. 3 simply by dividing the ordinate by the magnetic field of 18 kOe. However, more accurate Hall constants may be obtained from the slope of the field dependence curves shown in Fig. 4. This is clearly the case for the field in a ⟨111⟩ direction. From Fig. 4 and other supporting data, we deduce that

$$R_{H\langle 100\rangle}=14.4\times10^{-12}, \tag{3.1a}$$

$$R_{H\langle 111\rangle}=83.1\times10^{-12}, \tag{3.1b}$$

$$R_{H\langle 110\rangle}=11.9\times10^{-12}, \tag{3.1c}$$

expressed in units of volt cm/abampere gauss. For comparison, we note that the free-electron value is $R_{H_0}=7.4\times10^{-12}$. We shall relate the first two of these numbers to geometrical properties of the FS in Sec. IV. Open orbits occur for H along ⟨110⟩ and prevent a meaningful geometrical interpretation of[16] $R_{H\langle 110\rangle}$.

Data of a similar nature to that discussed above was taken for ten other "longitude" angles ϕ. To achieve better resolution, the full scale on the recorder was limited to "latitude" changes of 50°; and, on occasion, the full scale was reduced to 25°. Figure 5 shows the resistivity and transverse-even data measured between $\theta=+50°$ and $\theta=0°$ when $\phi=6.4°$. The various peaks seen in Fig. 5(a) appear as the magnetic field crosses magnetoresistance ridges, which lie on great circles or arcs of great circles on the unit sphere. Above each peak is indicated the net direction of the open orbits, perpendicular to the great circle on which the field lies. The method of assignment of these peaks is taken up in the next section where the transverse-even voltage is reviewed. The peaks labeled [111], $[01\bar{1}]$, and [101] constitute the principal behavior in this region, while the peaks [221] and [331] are some of the higher order open orbits reported earlier.[3] Small peaks too fine to reproduce in the figure were observed in the interval between the $[01\bar{1}]$ and [101] peaks. This is due to the "fuzz" surrounding the two-dimensional region centered on the $[1\bar{1}\bar{1}]$ direction. The field dependence of the peaks corresponds nearly to H^2 while that of the valleys or plateaus corresponds to saturation.

C. Higher Order Open Orbits, and Fine Structure

In order to exhibit the nature of higher order open orbits and other fine structure, two additional sets of data are shown in Figs. 6 and 7. These data were taken on expanded scales of 25° for the full "latitude" angle sweep and at increased sensitivity so as to accentuate the fine structure. Figure 6 corresponds to a "longitude"

angle $\phi=19.8$ and covers a "latitude" interval of $\theta=+77.5$ to $\theta=+52.5°$. The various peaks in this figure arise from "whiskers" that extend from the two-dimensional region surrounding the $[1\bar{1}0]$ axis. As before, the open-orbit directions giving rise to these magnetoresistance peaks are indicated above the peaks.

Figure 7 corresponds to fine structure generated by "whiskers" extending out from the two-dimensional region surrounding the $[00\bar{1}]$ direction. These data correspond to a "longitude" angle $\phi=13.1°$ and to a "latitude" angle range of $\theta=-25°$ to $\theta=-50°$. As before, the open-orbit directions giving rise to some of these peaks are indicated. A portion of these peaks are unmarked as they correspond to the "fuzz" surrounding this particular two-dimensional region. The appearance of a peak at $\theta=-33.75°$ on pairs 2 and 3 which is absent on pair 1 is of some academic interest. This peak is caused by the principal ridge whose open-orbit direction is $[1\bar{1}0]$. Ideally, if the current were along the [110] direction, and thus perpendicular to this open orbit, no trace of this peak should appear. The magnitude of the peaks observed in Figs. 7(b) and (c) may be used to deduce a current direction misalignment of about 1.5° from the [110] direction. Such a misalignment is inevitable and is, of course, not serious.

D. Stereographic Representation

If we idealize the observed behavior to regions of quadratic field dependence and to regions of saturation, then we may summarize our data conveniently in a stereographic representation. For clarity we exhibit only one quarter of the full stereogram. Figure 8 represents the principal ridges, substantially as reported earlier,[3] and indicates the multitude of higher order open orbits and "whiskers" as well. In this figure, the dotted regions and lines correspond to magnetic field directions that give rise to quadratic field dependence, while the clear regions correspond to magnetic field directions that give rise to saturation.

In order to more clearly represent the higher order open orbits, three additional stereograms, centered on [001], $[1\bar{1}0]$, and $[1\bar{1}\bar{1}]$, are presented in Figs. 9(a), 9(b), and 9(c), respectively. In most cases, the direction of the open orbit Ω that gives rise to the "whisker" is indicated. These figures have angular scales with which the extent of the two-dimensional regions and length of the various "whiskers" can be obtained. It is estimated that these figures are accurate to within $\pm 1°$.

We note the behavior in Fig. 9(c) in the vicinity of the point $[2\bar{2}\bar{3}]$. In that region, a medium-broad peak of resistivity appears that seems to come from two short "ridges" from open orbits along $[\bar{1}\bar{2}2]$ and [212] directions. That is, these "ridges," which appear as "whiskers" in Fig. 9(b) have *reappeared* in the angular interval near $[2\bar{2}\bar{3}]$. No other reappearance of this kind was found.

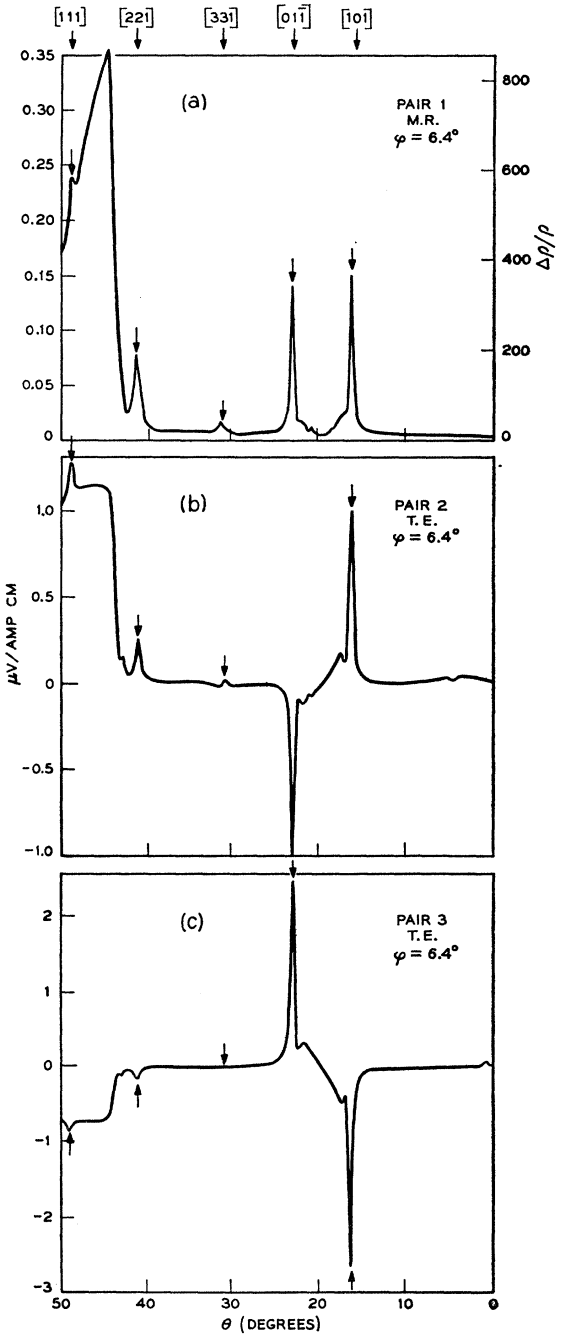

FIG. 5. Resistivity (a) and transverse-even voltages (b) and (c) versus θ for the "latitude" interval $50° \rightarrow 0°$ in the "meridian" plane $\phi=6.4°$. The ordinate is the relevant voltage divided by the sample current and by the probe separation. The magnetoresistance scale is given on the right of part (a). A number of features, indicated by arrows, are associated with the presence of specific open orbits whose net direction is shown marked at the top of the figure. Considerable fine structure that is impractical to resolve in the figure was observed in the region between the $[01\bar{1}]$ and [101] directions.

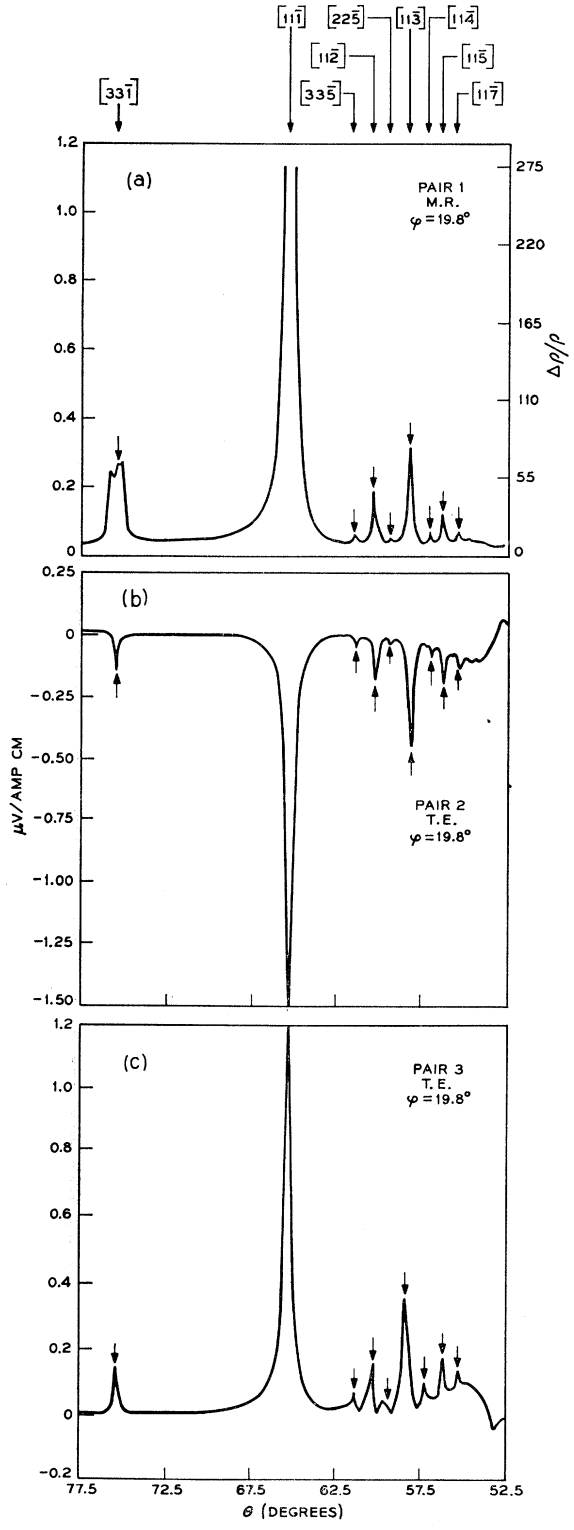

FIG. 6. Resistivity (a) and transverse-even voltages (b) and (c) versus θ for the "latitude" interval 77.5° → 52.5° in the "meridian" plane $\phi=19.8°$. The sensitivity in part (a) was so high that portions of the central spike were off scale. The ordinate is the relevant voltage divided by the sample current and by the probe separation. A magnetoresistance scale is given on the right of part (a). A number of features, which are indicated by arrows, are associated with the presence of specific open orbits whose net direction is shown marked at the top of the figure.

IV. THEORETICAL INTERPRETATION

A. Analysis of the Data

In the analysis of our galvanomagnetic data for Cu, we employ the theoretical interpretations arrived at by LAK[10] and LP.[11] The principal behavior of galvanomagnetic data and its connection with geometrical properties of the Fermi surface derived by these authors are by now well known.[13,19,20] Table I summarizes the essential features of the basic theory that we need for our study of Cu. In particular, a large value of the resistivity ρ, proportional to H^2, is attributed to the presence of a band of open orbits on the FS with a common net direction. The determination of the magnetic field directions which give rise to open orbits on the FS and the associated open-orbit direction, designated by the unit vector $\mathbf{\Omega}$, is basic to a determination of the FS shape. The open-orbit direction $\mathbf{\Omega}$ is obtained most simply by measuring the components of the electric field even in the magnetic field.

TABLE I. Five types of high-field behavior of the galvanomagnetic properties of metals and their relationship to "electron" or "hole" orbits. n is the number of carriers/atom; n_e is the number of "electrons"/atom; and n_h is the number of "holes"/atom.

Type	Nature of orbits	Behavior of resistivity in high magnetic field	Behavior of Hall constant in high magnetic field
I	All closed ($n_e \neq n_h$)	$\rho \to$ saturate	$R_H \propto n^{-1}$
II	Negligible number of open orbits ($n_e \neq n_h$)	$\rho \to$ saturate	$R_H \propto (n_e - n_h)^{-1}$
III	Open orbits in only one direction	$\rho \propto B + AH^2 \cos^2\alpha$[a]	$R_H \to$ const[b]
IV	Open orbits in more than one direction	$\rho \to$ saturate	$R_H \propto H^{-2}$
V	All closed ($n_e = n_h$)	$\rho \to H^2$[c]	$R_H \to$ const[b]

[a] α is the angle between the current $\mathbf{j}$ and the open orbit direction $\mathbf{\Omega}$.
[b] R_H is not related to the number of carriers in any simple manner.
[c] $\rho \to$ saturate if magnetic field is along current direction.

$$\mathbf{E}_e = \tfrac{1}{2}[\mathbf{E}(\mathbf{H}) + \mathbf{E}(-\mathbf{H})], \tag{4.1}$$

since the dominant part of $\mathbf{E}_e$ is expressed as[4]

$$\mathbf{E}_e = aH^2(\mathbf{\Omega}\cdot\mathbf{j})\mathbf{\Omega}. \tag{4.2}$$

Here $\mathbf{j}$ represents the current, and a is, essentially, a field-independent positive constant (in the high-field limit), depending in an involved way on the scattering and on the fraction of planes supporting the open orbits.

[19] A. B. Pippard, *Les Houches Lectures on Low Temperature Physics* (Gordon & Breach, Science Publishers, Inc., New York, 1962).
[20] J. M. Ziman, *Electrons and Phonons* (Oxford University Press, New York, 1960), p. 492.

The resistivity ρ is already a measure of the electric-field component along the current direction. Consequently, by measuring the component of $\mathbf{E}_e$ in the two transverse directions, i.e., the transverse-even voltages, we can determine the electric-field direction, and thus from (4.2) the open-orbit direction $\mathbf{\Omega}$. This technique to determine $\mathbf{\Omega}$ works so long as $\mathbf{\Omega}\cdot\mathbf{j}\neq 0$, independent of the value of a, so long as a is not so small as to invalidate (4.2).

The voltage scales for the resistivity and transverse-even voltages in Figs. 5–7 have been chosen so as to facilitate the determination of the open-orbit direction. The indicated normalized voltage scales were derived from the measured voltages by dividing by the probe separation and by the current magnitude and were always taken with $H=18$ kOe. Let us represent the open-orbit direction $\mathbf{\Omega}$ by its components Ω_1, Ω_2, and Ω_3 along axes parallel to the probe directions, 1, 2, and 3, respectively. Then the normalized voltage scales of parts (a), (b), and (c) of Figs. 5–7 are given, respectively, by

$$v_1=b\Omega_1,\ v_2=b\Omega_2,\ v_3=b\Omega_3,$$

where the common scale factor $b\equiv aH^2\Omega_1$. In other words, the three indicated vlotages have *already* been scaled so as to be proportional to the open orbit direction, when it exists. Its existence and the validity of (4.2) are, in turn, signaled by the presence of a large value or a peak in the rotation curve for v_1.

To illustrate the use of such data, consider the three peaks at $\theta=+16°$ in Fig. 5. The three voltages are, respectively, $v_1=1.53$, $v_2=1.0$, $v_3=-2.7$. These three values give a representation of the open orbit direction in the *sample* coordinate system, Now, to a good approximation, pairs 1, 2, and 3 lie along the unit vector directions $[110]/\sqrt{2}$, $[\bar{1}12]/\sqrt{6}$, and $[\bar{1}1\bar{1}]/\sqrt{3}$. Thus, the direction of the open orbit has the approximate crystallographic orientation $[2.24, -0.06, 2.38]$, which on normalization yields $\mathbf{\Omega}=[0.69, -0.018, 0.72]$ very close to the value $[101]$ indicated in Fig. 5.

With the aid of transverse-even voltages present in Figs. 2(b) and 2(c), the precise relation of the sample axes to the crystallographic axes can be determined. After including this refined relationship, the three even voltages, one for each sample pair, were used to compute proposed open-orbit directions in terms of crystallographic axes. Since the raw data were available on punched cards, it was a simple matter to carry out the necessary computations with the aid of the computer.

Various cross checks are available for the determination of $\mathbf{\Omega}$ and are especially valuable for the weaker signals for which Eq. (4.2) does not accurately apply. Of course, the simplest such cross check is merely to ensure that the proposed open-orbit direction $\mathbf{\Omega}$ lies perpendicular to $\mathbf{H}$. In addition, we have exploited the fact that the one-dimensional regions lie on great circles or arcs thereof by making up a useful table in the following way: First, for each rotational measurement we determine the "longitude" angle ϕ very accurately by

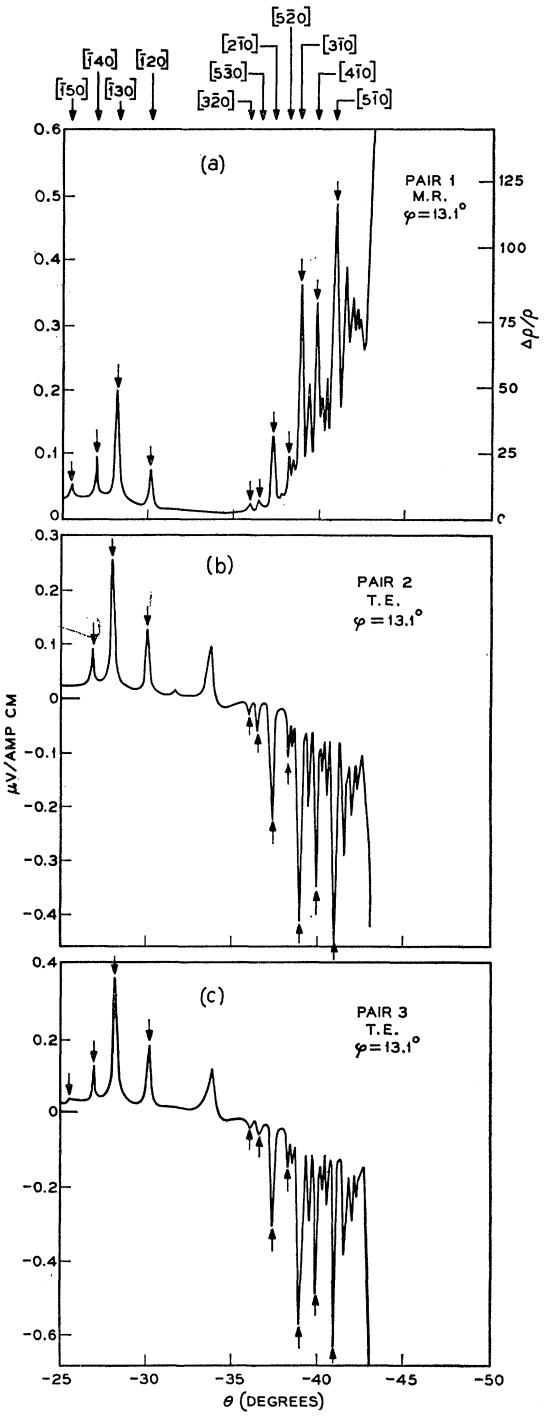

FIG. 7. Resistivity (a) and transverse-even voltages (b) and (c) versus θ for the "latitude" interval $-25°\rightarrow-50°$ in the "meridian" plane $\phi=13.1°$. The sensitivity in parts (a), (b), and (c) was so high that portions of the $[00\bar{1}]$ two-dimensional region ($\theta=-43°\rightarrow-50°$) were off scale. The ordinate is the relevant voltage divided by the sample current and by the probe separation. A magnetoresistance scale is given on the right of part (a). A number of features, which are indicated by arrows, are associated with the presence of specific orbits whose net direction is shown marked at the top of the figure.

focusing attention on the "latitude" angle differences between several of the identifiable, principal ridges. Second, predictions are made, again with the aid of the computer, of various "latitude" angles where the intersections of numerous great circles with the "meridian" plane occur. In this way, a table of hypothetical open-orbit directions was built up together with the "latitude" angle at which these open orbits would, if present at that "longitude," give rise to a magnetoresistance peaks in the observed data. Such a table has been of considerable value in sorting out assignments to many of the smaller amplitude "whiskers." Finally, the open-orbit assignments from one "meridian" plane were correlated and integrated with those of neighboring "meridian" planes to eliminate any lingering uncertainties and to achieve over-all consistency.

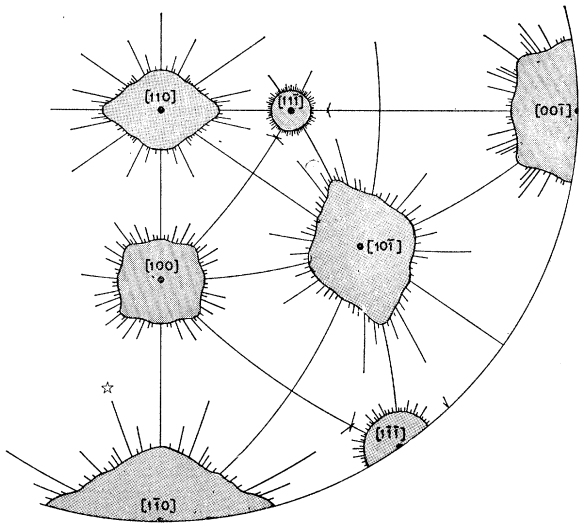

FIG. 8. Stereographic representation of data. The lines (one-dimensional regions) and the dotted areas (two-dimensional regions) represent regions for which the resistivity rises essentially as H^2. The clear area and symmetry points ⟨100⟩ and ⟨111⟩ represent regions for which the resistivity saturates. The star designates the higher order open orbit [11$\bar{3}$] which is examined in Sec. IV.

Higher Order Open Orbits

It is interesting that the observed family of open orbits are in reasonable agreement with those predicted by the elementary notion of higher order open orbits.[3,21] Let us imagine that the FS for Cu consists of a network of "undulating" cylinders along ⟨111⟩ directions. The observed data suggests that these cylinders are shaped so as to support ⟨111⟩-directed open orbits, which we call primary. Additional open orbits that may be possible follow from combinations of the primary directions in various arrangements. For example, if we combine a [111]- and a [1$\bar{1}\bar{1}$]-directed primary orbit, the net direction is [200]; hence, we say that ⟨100⟩-

[21] J. R. Klauder and J. E. Kunzler, J. Phys. Chem. Solids **18**, 256 (1961).

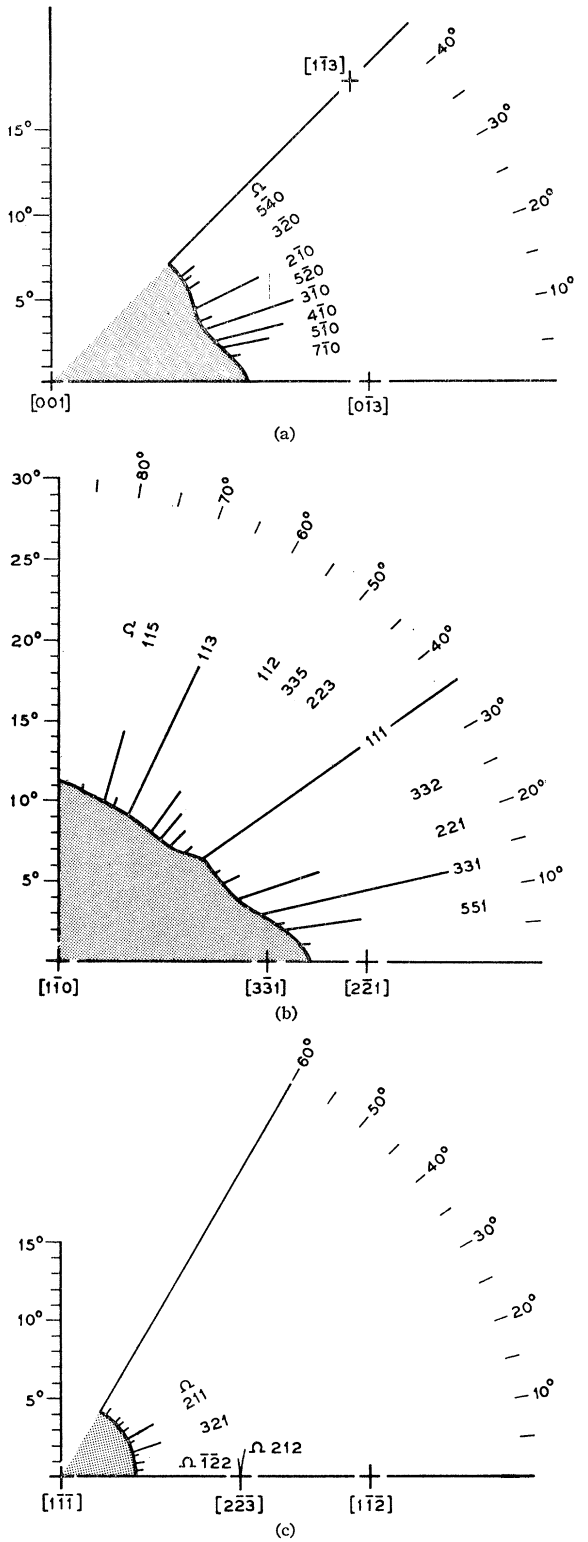

FIG. 9. Expanded partial stereograms centered on three principal axes: (a) [001]; (b) [1$\bar{1}$0]; (c) [1$\bar{1}\bar{1}$], respectively. For most of the "whiskers," the pertinent open-orbit direction **Ω** is indicated. The extent of the whiskers and two-dimensional region can be determined from the angular scale on the ordinate.

TABLE II. Potential open-orbit directions up to sixth order based on ⟨111⟩-directed primary open orbits. All orbits except ⟨135⟩ are observed in copper.

Order	Family of possible open-orbit directions
1	⟨111⟩
2	⟨100⟩, ⟨110⟩
3	⟨113⟩, ⟨133⟩
4	⟨012⟩, ⟨112⟩, ⟨122⟩
5	⟨115⟩, ⟨135⟩, ⟨155⟩, ⟨335⟩, ⟨355⟩
6	⟨013⟩, ⟨023⟩, ⟨123⟩, ⟨223⟩, ⟨233⟩

directed second-order open orbits are possible. Likewise ⟨110⟩-directed second-order open orbits are also possible In fact, these three types of open orbits are responsible for the principal magnetoresistance data observed in Cu.[3]

Still higher order open orbits correspond to many of the observed "whiskers." We give in Table II a list of the potential open-orbit directions predicted by this simple scheme up to sixth order. All of these orbits are observed and identified except ⟨135⟩. While the increasing order of the potential open orbit is no guarantee of a decreasing relative strength, it is rather gratifying that, to a first approximation, the indicated orbits, when they occur, have a strength and extent that decreases with increasing order.

B. Model of the Fermi Surface

The fundamental features of the FS of Cu have been known since the classic analysis of Pippard on the anomalous skin effect.[5] Early magnetoresistance studies, which concentrated on the principal ridges from open orbits along ⟨111⟩, ⟨100⟩, and ⟨110⟩ directions, substantiated the essential features of Pippard's model. Information of a quantitative nature regarding the Fermi surface can be derived from the Hall constant for certain orientations and from the angular extent of various one- and two-dimensional regions.

According to LP, the numerical value of the Hall constant has geometrical significance only for those field orientations that give rise to a negligible fraction of planes supporting open orbits. In such cases, the Hall constant is given by

$$R_H = R_{H_0}/\Delta n,$$

where R_{H_0} is the free-electron value and Δn is a geometrically determined factor representing the number of carriers per atom acting as "electrons" less those acting as "holes." In particular, if the z axis is chosen parallel to the magnetic field, then in suitable units we may write

$$\Delta n = \int dP_z \oint P_x dP_y$$

$$= \int dP_z \{S_e(E_f,P_z) - S_h(E_f,P_z)\}.$$

In the first form of this equation, the contour integral is to be evaluated around the several orbits that arise in each plane P_z. This contour integral just measures the enclosed area for electron-like carriers, S_e, and the negative of the enclosed area for hole-like carriers, S_h, leading to the second form for Δn. The second relation may, by adding and subtracting electron-like areas, be re-expressed as

$$\Delta n = V_e - \Delta(BZ)_h,$$

where V_e is the usual momentum space volume of occupied states and $\Delta(BZ)_h$ is that volume of the Brillouin zone bounded by planes normal to the magnetic field, within which the carriers effectively behave as holes. In this sense, it is seen that the geometrical content of the Hall constant for a particular field orientation is contained in the "turning points," those P_z planes which are boundary planes between planes of "electron"- and "hole"-like character.

In Cu the conditions for geometrical significance of the Hall constant are fulfilled for magnetic fields along the symmetry axes ⟨100⟩ and ⟨111⟩ and in the clear regions of the stereogram Fig. 8. In the clear regions, however, *no* open orbits occur on any momenutm planes, so no hole-like orbits can exist. Consequently, $\Delta(BZ)_h = 0$, and if we choose units such that $V_e \equiv 1$, then $R_H = R_{H_0} = 7.4 \times 10^{-12}$ volt cm/abamp G, the free-electron value. This value is in good agreement with the observed behavior, except in the close proximity of one- and two-dimensional regions. Such deviations may originate in the lack of high-field conditions existing for all carriers as is the case when extended orbits are present.

On the other hand, hole-like carriers do exist for field directions ⟨100⟩ and ⟨111⟩ so that their Hall constants differ from R_{H_0}. We have examined phenomenological FS's for Cu and determined theoretical Hall constants with the aid of a computer, by means of a program described elsewhere.[16] Our attention has been devoted to the FS expression given recently by Roaf[8] to fit Shoenberg's de Haas–van Alphen data[7] and Pippard's anomalous-skin-effect data,[5] and to an earlier one of Garcia-Moliner[6] that only fit Pippard's original data. Both formulas are given by tight-binding–type Fourier-series expressions with different sets of coefficients and are suitable to numerical studies. These series are fully discussed by Roaf, and we shall not repeat that discussion here.

Table III summarizes the experimental and theoretical values for the geometrical factor Δn. As is customary, we have included the experimental and theoretical values for field directions ⟨110⟩, although for these directions a non-negligible fraction of planes supporting open orbits do in fact exist.[16] Following previous procedure,[16] we have regarded such planes as electron-like in order to determine the theoretical prediction. However, we re-emphasize that, besides the "valleys," a meaningful comparison between theory and experi-

TABLE III. Geometrical factor Δn entering the Hall constant as found experimentally and predicted theoretically. The Hall constant itself is given as $R_H = 7.4 \times 10^{-12}/\Delta n$ volt cm/abamp-G.

Field direction	Experimental	Theoretical CU VI[a]	Theoretical GM[b]
"Valleys"	1.00 ±0.01	1.00	1.00
⟨100⟩	0.51 ±0.01	0.51	0.71
⟨111⟩	0.089±0.003	0.068	0.32
⟨110⟩	0.62 ±0.01	0.51	0.72

[a] D. J. Roaf, Phil. Trans. Roy. Soc. **A255**, 135 (1962).
[b] F. Garcia-Moliner, Phil. Mag. 3, 207 (1958).

ment exists only for the directions ⟨100⟩ and ⟨111⟩. From the data for these directions, we conclude that the theoretical predictions of Roaf's model CU VI are remarkably consistent with our observed Hall constants. This is especially true when account is taken of the extreme sensitivity of the experimental and theoretical values for ⟨111⟩ directions. The values derived from the FS expression of Garcia-Moliner (GM) are in poor agreement with our present Hall constant data.

As our final comparison of our data with FS models, we examine further one of the higher order open orbits, the tertiary open orbit [11$\bar{3}$], which is starred in the stereogram 8. From the equivalent arc labelled [113] in Fig. 9(c), we learn that this higher order open orbit continues past the two-dimensional region, which ends at about 10°, and extends out to about 20° from the [1$\bar{1}$0] axis. In order to compare such information with the FS model, we have sought for similar angular behavior of ⟨113⟩-directed open orbits with the aid of the computer and our general purpose program. In this study, the range of momentum planes normal to the

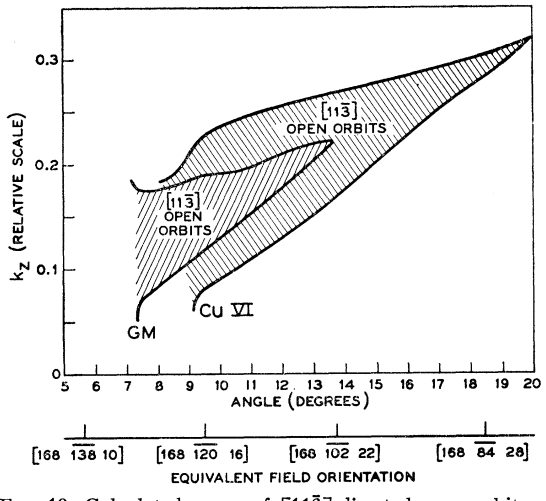

FIG. 10. Calculated range of [11$\bar{3}$]-directed open orbits supported by models of Fermi surfaces. The abscissa represents the angle measured in the (11$\bar{3}$) plane between the magnetic field direction and the [1$\bar{1}$0] direction, while the ordinate is the distance from the zone center Γ to various momentum planes perpendicular to the field on a scale in which $\Gamma - X$ is one unit. The shaded regions show the range of momentum planes for which the Garcia-Moliner (GM) and Roaf's best (CU VI) FS models support [11$\bar{3}$]-directed open orbits.

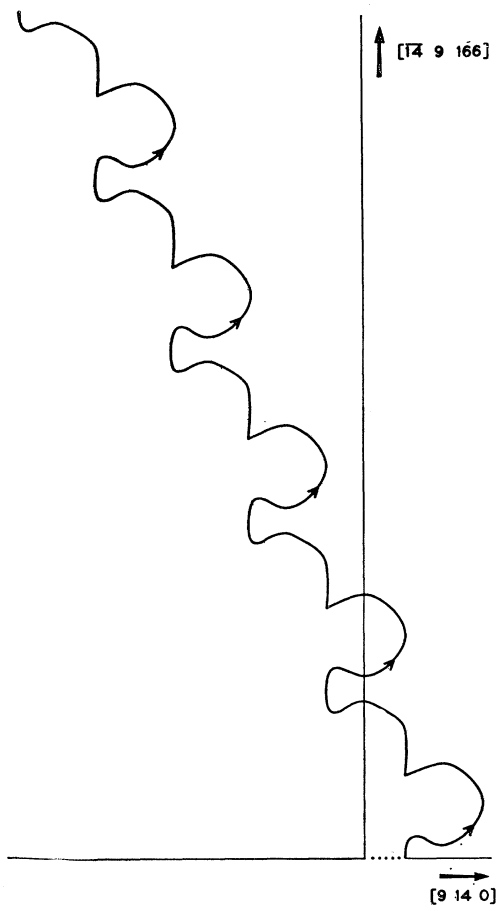

FIG. 11. Example of a calculated higher order open orbit with a net [11$\bar{3}$] direction. This open orbit lies in the CU VI shaded region of Fig. 10 at $k_z = 0.15$, and an angle of 12°. (For this plane and angle, the GM model FS supports no [11$\bar{3}$] open orbits.)

field which carry [11$\bar{3}$]-directed open orbits was found for a number of field orientations in the (11$\bar{3}$) plane. A summary of that study appears in Fig. 10. This figure shows, for two different FS models, the range of momentum planes versus the angle between the [1$\bar{1}$0] axis and the field direction. On this scale for the ordinate, the distance from the zone center Γ to a {100}-zone face is one unit.

From Fig. 10 it can be seen that the CU VI model supports ⟨113⟩ open orbits out to 20°, as experimentally observed, while for the GM model they extend to less than 14°. On the other hand, at about 9½° for the CU VI model and at 7½° for the GM model, the fraction of planes supporting open orbits increases dramatically, as is indicated by the opening downward of both envelopes. We interpret this dramatic change as characterizing the edge of the two-dimensional boundary. On these grounds, the 9½° value for the CU VI model is in very good agreement with the experimental value of 10°, especially in view of the accuracy with which these values can be deduced from our data.

In the manner of Ref. 16, Fig. 11 shows one of the

[11$\bar{3}$]-directed open orbits supported by the model CU VI traced out in the compilation of the data for Fig. 10. This orbit lies just inside the shaded region at a relative $k_z=0.15$ and at an angle 12° between the field and [1$\bar{1}$0] axis.

Based on the above arguments, we find that Roaf's phenomenological FS model CU VI is in good accord with our galvanomagnetic measurements with respect to Hall constant values and angular extent of various one- and two-dimensional regions.

PHYSICAL REVIEW VOLUME 141, NUMBER 2 JANUARY 1966

Core-Polarization Contribution to the Knight Shift in Beryllium Metal*

WEI-MEI SHYU, G. D. GASPARI,† AND T. P. DAS
Department of Physics, University of California, Riverside, California
(Received 1 June 1965)

Direct and core-polarization contributions to the Knight shift in beryllium metal were calculated at a number of symmetry points near the Fermi surface. The direct contribution was evaluated using wave functions for the conduction electrons by the orthogonalized-plane-wave method. The contribution of the core electrons was determined using the moment-perturbation (MP) method developed in an earlier paper. The accuracy of the MP method was rechecked by calculating the core contribution to the hyperfine coupling constant in the $^3P_2$ state of the beryllium atom. Good agreement was obtained with the result of an earlier self-consistent-field calculation by Goodings. For the Γ_4^- level, the direct and core contributions to the Knight shift are 0.01536 and 0.00258%, respectively. For the two degenerate levels of H_1, the direct contributions both vanish while the core-polarization contributions are −0.00061 and −0.00001%. These results lead to the conclusion that core-polarization effects alone can not explain the near-vanishing Knight shift observed experimentally in beryllium metal. Some other contributions such as those from various orbital mechanisms would therefore have to be considered.

I. INTRODUCTION

A NUMBER of recent papers[1–4] have dealt with the theory of the Knight shift in beryllium metal. Earlier measurement by Knight[1,5] showed that the Knight shift was less than 0.002%; that is, essentially zero within experimental error. The theoretical investigations, on the other hand, while they differ quantitatively in their predictions, all lead to finite values of the Knight shift which are beyond the range of experimental error.

Since beryllium is a light metal with only one core state, one would expect an analysis of the Knight shift to be relatively easier compared to heavier metals. In heavier metals the spin-orbit and other relativistic effects and the problem of orthogonality to core states lead to complications in the calculation of the wave functions for conduction electrons. It is therefore important to understand the reasons for the disagreement between theoretical and experimental results for Be. The first source that comes to mind is possible inaccuracies in the wave function employed to make the theoretical estimates of Knight shift in earlier papers. Wood and Milford[3] employed augmented plane-wavefunctions based on earlier calculations by Jacques.[6] They assumed a spherical Fermi surface and found that the Knight shift is appreciable. A spherical Fermi surface was also assumed by Pomerantz and Das[2] who used an orthogonalized-plane-wave (OPW) calculation and found the Knight shift to be substantial. Townes, Herring, and Knight[1] obtained their Knight shift result from Herring and Hill's OPW calculation.[7] Herring and Hill determined the energy levels at a number of points and lines in **k** space but did not include many OPW functions in their calculation owing to the lack of computing facilities at the time. The most recent calculations on the band structure and Fermi surface of Be metal are due to Loucks and Cutler[8] and Loucks,[9] who made a careful study of the potential to reach a certain degree of self-consistency and obtained energy levels at a number of points using fairly high order secular equations. They found quite good agreement with the available de Haas–van Alphen data[10] and soft x-ray spectro-

* Supported by the National Science Foundation.
† Present address: Department of Physics, University of Rochester, Rochester, New York.
[1] C. H. Townes, C. Herring, and W. D. Knight, Phys. Rev. **77**, 852 (1950).
[2] M. Pomerantz and T. P. Das, Phys. Rev. **119**, 70 (1960).
[3] V. E. Wood and F. J. Milford, J. Phys. Chem. Solids **23**, 160 (1962).
[4] W. Schneider, L. Jansen, and L. Etienne-Amberg, Physica (Netherlands), **30**, 84 (1964).
[5] W. D. Knight, *Solid State Physics*, edited by F. Seitz and D. Turnbull (Academic Press Inc., New York, 1956), Vol. 2.
[6] R. Jacques, Cahiers de Phys. **70**, 1 (1956); **71-72**, 23 (1956); **75-76**, 17 (1956).
[7] C. Herring and A. G. Hill, Phys. Rev. **58**, 132 (1940).
[8] T. L. Loucks and P. H. Cutler, Phys. Rev. **133**, A819 (1964).
[9] T. L. Loucks, Phys. Rev. **134**, A1618 (1964).
[10] B. R. Watts, Phys. Letters **3**, 284 (1963).